

Thermally Induced Water Flux in Soils

Zhen Liu, Bin Zhang, Xiong (Bill) Yu, Junliang Tao, Ye Sun, and Quan Gao

A comprehensive study is presented for the formulation of thermally induced water flux. For conditions without ice lenses, either frozen or unfrozen conditions, a theory is proposed to address the underestimation of water flux by the model of Philip and de Vries. In addition, experiments with a modified capillary rise method are proposed to calculate a gain factor that accounts for this underestimation. For thermally induced flux in frozen soils with ice lenses, a theoretical formulation is derived for the segregation potential, which is the key parameter in the model of Konrad and Morgenstern. This theoretical formulation, which is lacking in previous research, is expressed in a simple mathematical form and can be conveniently used for accurate prediction of segregation potential. The validity of the theory is proved with reported data, and more auxiliary relationships are provided for accurately predicting the segregation potential with the proposed formulation.

Soils are susceptible to multiphysical phenomena because of their nature as a porous material consisting of a porous skeleton and pore fluids. They are susceptible because this distinct nature provides favorable conditions for energy transfer, water migration, and geo-mechanical responses, which correspond to thermal, hydraulic, and mechanical fields, respectively. These physical processes are more or less coupled in nature, so it is difficult to separate one from the others. But a single physical phenomenon can be analyzed without significantly affecting the analysis results when the couplings between different physical fields are weak enough. This analysis is in fact what geotechnical engineers mostly do when they are dealing with issues related to soils. However, in some cases, the couplings between some physical processes are very strong. Typical examples include the behavior of energy piles and their influence on soil properties, energy harvesting from soils, and the influence of thermal changes on soil properties. More concern has been shifted from individual physical phenomena to coupled multiphysical processes because of emerging needs in geotechnical practice and advances in multiphysics research.

The couplings between different physical fields, as shown in Figure 1, could be very complicated. Many multiphysical phenomena are triggered by a change in the thermal field. This change serves as an excitation, similar to an external force in the mechanical field, and gives rise to changes to the whole system in terms of a multiphysical process. For example, thermal changes can alter soil compressibility and shear strength (mechanical), induce water migration, and change

hydraulic properties (hydraulic). These are the typical couplings from the thermal field to the mechanical and hydraulic fields, respectively. These changes in the mechanical and hydraulic fields will in return exert reacting forces on the thermal field. For example, heat transfer can be promoted by energy convection through migratory water, and thermal properties such as heat capacity and thermal conductivity can be changed through variations in the structure and composition of soils. The reacting forces represent the couplings from the other two physical processes to the thermal field. The couplings from the thermal field to the other fields are usually strong couplings. Among these couplings, thermally induced water flux is especially significant and thus of special interest. This process of water transfer due to temperature gradients is critical to many multiphysical processes in soils. When the phase change of water (freezing or thawing) is involved, a multiphysical phenomenon could be more complicated and the significance of the thermally induced water flux can be seriously exaggerated. One typical example is frost heave, in which water is sucked from deeper positions to an advancing frost front because of temperature changes on the ground surface.

Various methods have been proposed to formulate thermally induced water flux. Philip and de Vries developed a theory based on thermodynamics to explain moisture movement in porous materials under temperature gradients (1). Dirksen and Miller used similar concepts but with emphasis on the mechanical analysis (2). Studies from physical chemistry emphasized the influence of surface tension (3–5) and called for attention to the role of the water vapor adsorption process (6, 7). Coussy described the transport of water and vapor as the result of differences in density, interfacial effects, and drainage due to expelling, cryosuction, and thermomechanical coupling (8). A few researchers have also described the transport of water in response to a temperature gradient by using the theory of nonequilibrium thermodynamics (9–12). However, most multiphysics simulations based on continuum mechanics are developed on the basis of the theory proposed by Philip and de Vries (13–15). This model has also been applied to freezing soils without ice lenses (16, 17).

The formulation of thermally induced water flux in frozen soils may be different from that without a phase change of water. Dirksen and Miller (2) found that the rate of mass transport within the frozen soil exceeded by several orders of magnitude that which could be accounted for as vapor movement through the unfilled pore space. It was therefore concluded that the flux must have taken place in the liquid phase by a factor at least 1,000 times faster than that predicted by Philip and de Vries (1) and subsequent researchers. Miller proposed the rigid ice model, in which ice pressure was nonzero and was related to water pressure through the Clapeyron equation (18). The movement of ice content as a function of mean curvature occurred in the form of ice re-gelation (19). Gilpin developed a theory by assuming that the movement of water in the liquid layer was totally controlled by the normal pressure-driven viscous flow (20). Dash proposed that the driving force was attributed to the lowering of the interfacial free energy of a solid surface by a layer of the

Z. Liu, Bingham 256, X. Yu, Bingham 206, and J. Tao, Bingham 203B, Department of Civil Engineering, and Y. Sun, Bingham 203C, and Q. Gao, Bingham 211A, Department of Electrical Engineering and Computer Science, Case Western Reserve University, 2104 Adelbert Road, Cleveland, OH 44106-7201. B. Zhang, Department of Civil Engineering, China University of GeoSciences, Beijing 100086, China. Corresponding author: X. Yu, xxy21@case.edu.

Transportation Research Record: Journal of the Transportation Research Board, No. 2349, Transportation Research Board of the National Academies, Washington, D.C., 2013, pp. 63–71.
DOI: 10.3141/2349-08

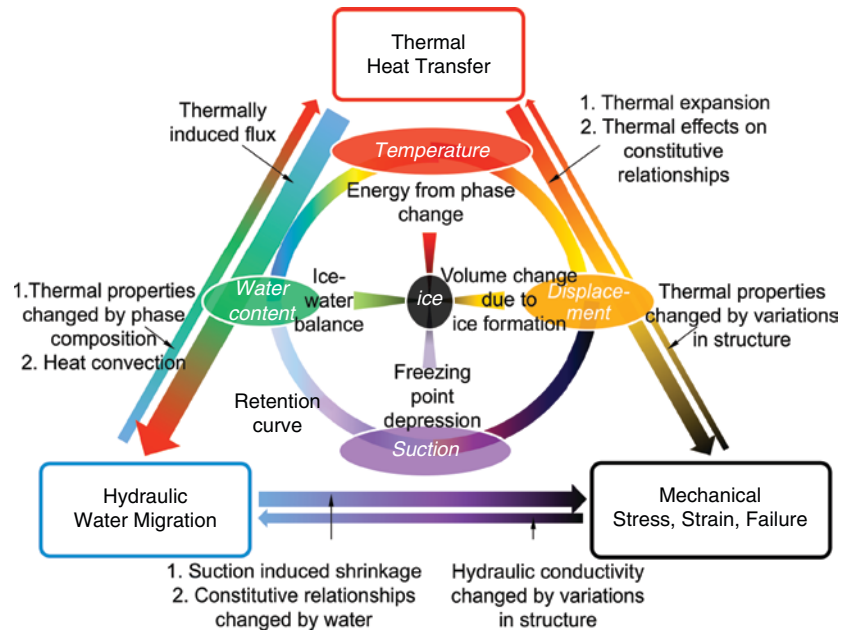


FIGURE 1 Couplings between physical fields in soils.

melted material; this condition occurs for all solid interfaces that are wetted by the melted liquid (21). There are other practical models, such as the one by Konrad and Morgenstern (22–24). In this model, the coupling was simplified by introducing an experimental relationship in which the rate of water migration was proportional to the temperature gradient in the frozen fringe.

Among the previously named methods, the model proposed by Philip and de Vries (1) and that by Konrad and Morgenstern (22–24) have gained popularity for simulations without and with ice lenses, respectively. A comprehensive study is presented here for the formulation of thermally induced water flux. For conditions without ice lenses, either frozen or unfrozen, a theory is proposed to address the underestimation of water flux by the model of Philip and de Vries (1). In addition, experiments with a modified capillary rise method (CRM) were proposed to calculate a gain factor accounting for the underestimation. For the thermally induced flux in frozen soils with ice lenses, the theoretical formulation for the segregation potential, which is the key parameter in the model of Konrad and Morgenstern (22–24), is derived. This theoretical formulation, which is lacking in previous research, is expressed in a simple mathematical form and can be conveniently used for accurate prediction of the segregation potential. The validity of the theory is proved with reported data. More auxiliary relationships are provided for accurate prediction of the segregation potential.

CONDITIONS WITHOUT ICE LENSES

Theoretical Background

The model of Philip and de Vries was established on the basis of thermodynamics (1). The derivation began from Darcy’s law, as follows:

$$\bar{j} = -\frac{K}{g} \nabla \Phi \tag{1}$$

where

- \bar{j} = gravimetric liquid flux,
- K = hydraulic conductivity,
- Φ = total potential (Pa), and
- g = gravitational constant.

In the original derivation, Φ was assumed to include matric potential and gravitational potential:

$$\Phi = \psi_m + \psi_g \tag{2}$$

where ψ_m is the matric potential and ψ_g is the gravitational potential. It is well known that ψ_m is related to water content in partially saturated soils (or partially frozen soils). This relationship is called the soil water characteristic curve. Philip and de Vries believed that the thermally induced water flux is attributed to the nonisothermal soil water characteristic curve (1). To be more specific, it stems from the temperature dependence of the surface tension of the water–vapor (or water–ice) interface.

$$\psi_m = \psi_m(\theta, \gamma(T)) \tag{3}$$

where

- θ = volumetric water content in partially saturated soils (or unfrozen water content in partially frozen soils),
- γ = surface tension of water–vapor interface in partially saturated soils (or water–ice interface in partially frozen soils), and
- T = temperature.

Substituting Equations 2 and 3 into Equation 1, the following equation for thermally induced flux was obtained:

$$\bar{j} = -\frac{K}{g} \frac{\partial \psi_m}{\partial \gamma} \frac{\partial \gamma}{\partial T} \nabla T - \frac{K}{g} \frac{\partial \psi_m}{\partial \theta} \nabla \theta - \frac{K}{g} \bar{i} \tag{4}$$

where \vec{i} is the unit vector in the direction of gravity. The matric suction can be formulated by using the Young–Laplace equation as follows:

$$\Psi_m = \frac{2\gamma \cos \phi}{r} \quad \text{or} \quad \frac{\partial \Psi_m}{\partial \gamma} = \frac{\Psi_m}{\gamma} \quad (5)$$

where ϕ is the contact angle and r is the pore radius.

So the thermally induced water flux can be expressed as

$$\vec{J} = -\frac{K}{g} \frac{\Psi_m}{\gamma} \frac{\partial \gamma}{\partial T} \nabla T - \frac{K}{g} \frac{\partial \Psi_m}{\partial \theta} \nabla \theta - \frac{K}{g} \vec{i} \quad (6)$$

Equation 6 is the mathematical formulation obtained by Philip and de Vries (1). In later implementations, the hydraulic conductivity due to temperature was mostly used, and isothermal soil water characteristic curves were employed. Hence Equation 6 can be reformatted:

$$\vec{J} = -\frac{K_T}{g} \nabla T - \frac{K}{g} \nabla \hat{\Psi}_m - \frac{K}{g} \vec{i} \quad (7)$$

where K_T is the hydraulic conductivity due to temperature, and $\hat{\Psi}_m$ is the matric potential in the isothermal characteristic curve. Accordingly, K_T is expressed as

$$K_T = K \frac{\Psi_m}{\gamma} - \frac{\partial \gamma}{\partial T} \quad (8)$$

Hydraulic conductivity due to temperature characterizes the ease with which water can move through pore spaces or fractures under the influence of temperature. However, experimental evidence has repeatedly indicated that the foregoing formulation underpredicts the influence of temperature on water migration (3, 25). The degree of underestimation was found to vary from soil to soil. As concluded by Nimmo and Miller (3), the temperature dependence in coarse-grained soils is about as strong as expected from the previous theory, whereas for fine-textured soils, it is significantly stronger. Figure 2

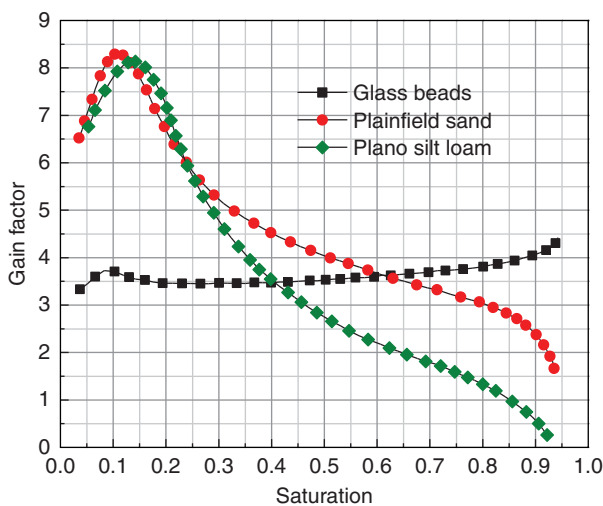


FIGURE 2 Gain factor versus water content for glass beads, Plainfield sand, and Plano silt loam (3).

illustrates the gain factors measured by Nimmo and Miller for gas beads, Plainfield sand, and Plano silt loam (3). In their study, the gain factor was proved to be dependent on water saturation. The gain factor was calculated with the nonisothermal soil water characteristic curve of the same soil. Tensiometers and a gamma-ray transmission system were employed for the experiments. Therefore, measurement of the gain factor requires special devices and precise control of the experiment. A gain factor such as 7 was used in some thermohydraulic studies (16, 26).

New Theory

Cary's summary held that surface tension, soil moisture suction, and kinetic energy changes with the hydrogen bond distribution, as well as thermally induced osmotic gradients, should be responsible for the thermally induced water flow (27). Grant and Salehzadeh (4) claimed that the temperature sensitivities of the wetting coefficient could contribute to the underestimation made by the theory of Philip and de Vries (1). To take these factors into account, the definition of the total potential of soils is as follows:

$$\Phi = \Psi_m + \Psi_o + \Psi_g + \Psi_e + \Psi_a \quad (9)$$

where

Ψ_o = osmotic potential,

Ψ_e = envelope potential resulting from overburden pressures, and

Ψ_a = pneumatic potential.

Among these components, it can be seen that matric potential and osmotic potential are the two potential components that depend on temperature. The osmotic potential can be expressed as

$$\Psi_o = icRT \quad (10)$$

where

i = osmotic coefficient (van't Hoff factor),

c = concentration of solute, and

R = universal gas constant.

So the temperature influence on soil potential based on Equation 9 can be formulated as follows:

$$\frac{d\Phi}{dT} = \frac{\partial \Psi_m}{\partial \gamma} \frac{\partial \gamma}{\partial T} + \frac{\partial \Psi_m}{\partial \phi} \frac{\partial \phi}{\partial T} + \frac{\partial \Psi_o}{\partial T} = \frac{\Psi_m}{\gamma} \frac{\partial \gamma}{\partial T} + \frac{\Psi_m}{\cos(\phi)} \frac{\partial \cos(\phi)}{\partial T} + icR \quad (11)$$

On the basis of Equation 11, the gain factor can be obtained:

$$G = 1 + \frac{icR\gamma - \gamma \tan \phi \frac{d\phi}{dT}}{\frac{d\gamma}{dT}} \quad (12)$$

The value of $(\partial \phi / \partial T)$ can be assumed to be 0.1 arc degree/ $^{\circ}\text{K}$ from the results reported by Neumann et al. (28) and Adamson (29), which is at least reasonable for many systems at temperatures between 5 arc

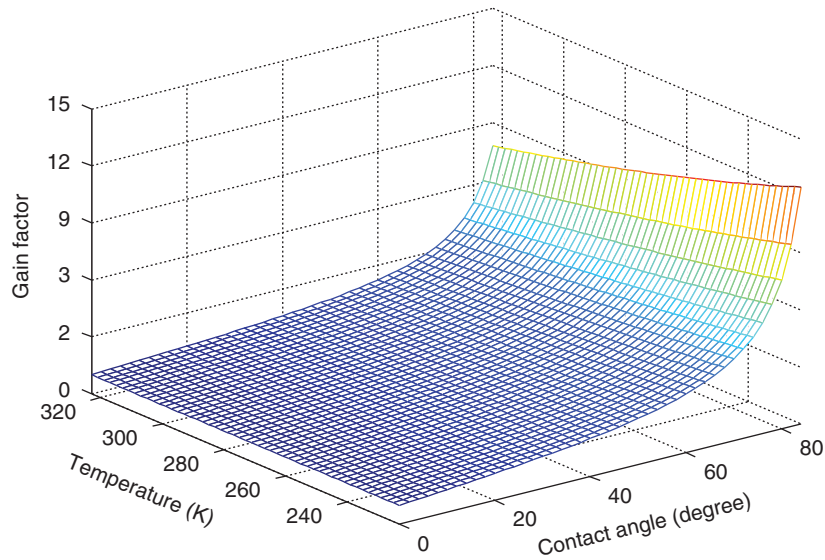


FIGURE 3 Gain factor versus temperature and contact angle.

degrees and 100 arc degrees (30). The surface tension is expressed as a function of temperature as follows:

$$\gamma = [75.6 - 0.1425(T - 273) - 2.38 \times 10^{-4}(T - 273)^2] \times 10^{-3} \left(\frac{N}{m} \right) \tag{13}$$

If the osmotic effect is negligible, the gain factor can be simplified as follows:

$$G = 1 + \frac{[75.6 - 0.1425(T - 273) - 2.38 \times 10^{-4}(T - 273)^2] \tan \phi}{81.65 + 272.73 \times 10^{-3}(T - 273)} \tag{14}$$

The gain factors calculated with Equation 14 are plotted in Figure 3. The calculated gain factors agree well with the measured data in Figure 2. As can be seen, the gain factor increases as the contact angle increases. When the contact angle is close to 90 degrees—that is, the soil has a nearly neutral wettability—the gain factor is extremely high. In contrast, the gain factor is 1 when a soil is completely wettable. This finding explains why glass beads, whose contact angle with water is very small, has a relatively low gain factor. To apply Equation 14 to multiphysics simulations, the contact angle needs to be measured. In this study, a modified CRM is presented for measuring the contact angle of soils.

Modified CRM

The influences of inertia and gravity were neglected in most of the previous CRM studies. Consequently, a simplified Lucas–Washburn equation is obtained in the following form (31, 32):

$$\underbrace{2\pi r \gamma \cos(\phi)}_{\text{surface tension}} - \underbrace{8\pi \eta h(t) \frac{\partial h(t)}{\partial t}}_{\text{viscous force}} = 0 \quad \text{or} \quad B - Chh' = 0 \tag{15}$$

where

- r = radius of capillary,
- γ = surface tension of interface between solid and test (imbibed) liquid,
- t = time,
- $h(t)$ = height of capillary rise at time t , and
- η = dynamic viscosity of test liquid.

The analytical solution to this simplified Lucas–Washburn equation predicts a linear relationship between the squared height of the imbibed liquid and time (31, 32):

$$h = \left(\frac{2B}{C} t \right)^{\frac{1}{2}} = \left(\frac{r \gamma \cos(\phi)}{2\eta} t \right)^{\frac{1}{2}} \tag{16}$$

The conventional CRM requires identifying a stage (viscous dominant) when the simplified Lucas–Washburn equation can satisfactorily describe the dynamics of capillary rise (33). However, it is possible that such a stage is very short or even does not exist. Even if such a stage exists, a part of the m^2 - t curve where its tangent has the least slope variation needs to be identified for linear regression (34). Thus implementation of the method involves numerous subjective factors. To improve the conventional CRM, the influence of gravity is considered:

$$\underbrace{2\pi r \gamma \cos(\phi)}_{\text{surface tension}} - \underbrace{8\pi \eta h(t) \frac{\partial h(t)}{\partial t}}_{\text{viscous force}} - \underbrace{\rho \pi r^2 g h(t)}_{\text{gravity}} = 0$$

or $B - Chh' - Dh = 0$ (17)

where ρ is the density of the test liquid. An analytical solution to Equation 17 was obtained by using MATLAB:

$$h = \frac{B}{D} \left\{ 1 - W \left[\exp \left(-1 - \frac{D^2}{BC} t \right) \right] \right\} \tag{18}$$

where W is the Lambert W-function. That is,

$$h = \frac{2\gamma \cos(\phi)}{\rho g r} \left\{ 1 - W \left[\exp \left(-1 - \frac{\rho^2 g^2 r^3}{16\gamma \eta \cos(\phi)} t \right) \right] \right\} \quad (19)$$

The preceding solution (height gain) is reformatted in the form of imbibed mass (mass gain):

$$m = \frac{2\pi r N \gamma \cos(\phi)}{g} \left\{ 1 - W \left[\exp \left(-1 - \frac{\rho^2 g^2 r^3}{16\gamma \eta \cos(\phi)} t \right) \right] \right\} \quad (20)$$

where N is the number of equivalent capillaries involved in a capillary rise process, and $\pi^2 r^5 N$ is usually referred to as the Washburn constant. A piecewise equation proposed by Barry et al. was used to approximate the Lambert W-function equation in this study (35).

Tortuosity was not included in the definition of apparent contact angle. According to Czachor (36), the tortuosity τ is the ratio of the actual path taken by a liquid moving through pores, \tilde{h} , to the distance between the starting and final heights, h (37, 38):

$$\tilde{h} = \tau h \quad (21)$$

$$\underbrace{2\pi \tilde{r} \gamma \cos(\tilde{\phi})}_{\text{surface tension}} - \underbrace{8\pi \eta \tau^2 h(t) \frac{\partial h(t)}{\partial t}}_{\text{viscous force}} - \underbrace{\rho \pi \tilde{r}^2 g \tau h(t)}_{\text{gravity}} = 0 \quad (22)$$

The term m_0 , which describes the mass absorbed on the balance before measurements, was added to the fitting functions (39). So the fitting equation can be formulated as follows:

$$m = m_0 + \kappa \{ 1 - W[\exp(-1 - \alpha t)] \} \quad (23)$$

where m_0 , κ , and α are fitting constants.

From Equation 23, water and another reference liquid are usually used to obtain contact angles. The test liquid used for reference is usually an organic solvent with low surface energy, such as hexane or pentane. Considering the comparatively high surface energy of soil particles and low surface tension of the reference liquid, the contact angle between the reference liquid and a soil is approximately zero. Then the apparent contact angle between water and soils can be calculated with κ (κ_w and κ_l) obtained by curve fitting:

$$\phi = \arccos \left(\frac{\kappa_w}{\kappa_p} \cdot \frac{\eta_w \rho_p^2 \gamma_p}{\eta_p \rho_w^2 \gamma_w} \right) \quad (24)$$

where

$$\begin{aligned} \kappa_{J,p}, \kappa_{J,w} &= \text{constants pertaining to pentane and water, respectively;} \\ \rho_p, \gamma_p &= \text{density and surface tension of pentane, respectively;} \\ &\text{and} \\ \rho_w, \gamma_w &= \text{density and surface tension of water, respectively.} \end{aligned}$$

The effective radius and number of capillaries were cancelled out.

For test liquids, water and pentane were used in this study. The density, surface tension, and viscosity of water are $1,000 \text{ kg/m}^3$, $71.79 \times 10^{-3} \text{ N/m}$, and $1.002 \times 10^{-3} \text{ N} \cdot \text{s/m}^2$, respectively; those of pentane are 626.2 kg/m^3 , $15.82 \times 10^{-3} \text{ N/m}$, and $0.24 \times 10^{-3} \text{ N} \cdot \text{s/m}^2$, respectively. An Ohio subgrade soil was used for the experiment.

Duplicate soil specimens were prepared by strictly following the same procedures described in the following paragraphs to ensure the similarity. A soil was poured into a tube standing upright on a table from the same height as the top of the tube. After the upper surface of the soil reached the top of the tube, the tube was vibrated with a small vibrator at a frequency of 55 Hz for 60 s. A metallic tool with a base and a vertically protruding pipe was used to accommodate the tube while it was on the vibrator. All soil specimens were put into a tube rack after vibration for transportation and testing.

A K100 tensiometer was used for the contact angle measurements (40). Here its electronic balance instead of the built-in modules is employed. As illustrated in Figure 4, a self-fabricated tube filled with a soil was attached to the electronic balance with a clip. The rigid clip was used to reduce the time of self-stability for the electronic balance. A glass vessel with a test liquid in it was placed on a lifting stage below the tube. During a measurement, the stage moved up until it was in contact with the sieve glued at the bottom of the tube. Measurement of the m - t curve was triggered when a contact was detected.

The glass tubes are 44.5 mm high and have an internal diameter of 5.75 mm and an outer diameter of 7.9 mm. The tubes were made of soda-lime glass because of its comparatively high fracture toughness. The same number of metallic sieves with an opening of $75 \mu\text{m}$ were prepared. These sieves were circular and had a diameter that was 1 mm bigger than the outer diameter of the tube. Each sieve was glued to the bottom of a tube, which was sanded beforehand. The glue was chosen because of its high temperature resistance and chemical resistance.

These procedures were designed and strictly followed during the experiments:

1. All tubes and vessels were rinsed with acetone and then dried before tests.
2. The soils for test were dried in an oven (80°C) for 24 h. Then the soil specimens were prepared by following the aforementioned procedures.
3. The tube was put into the chamber of the tensiometer as shown in Figure 4 and a rinsed vessel was filled with test liquid according to the requirement of the tensiometer.

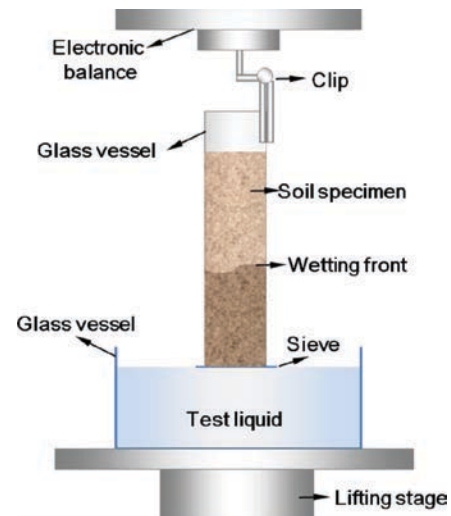


FIGURE 4 Instrument setup for CRM with Krüss 100 tensiometer.

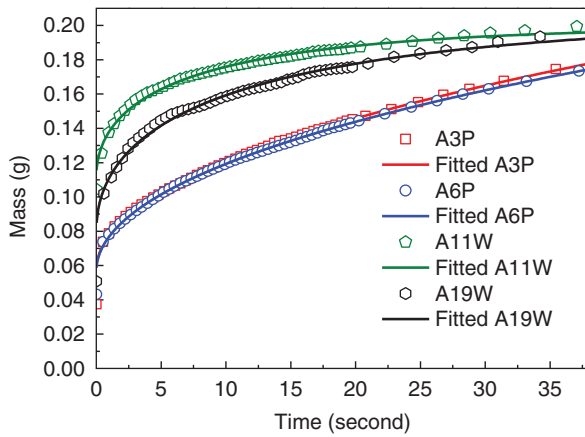


FIGURE 5 Comparison between measured and fitted $m-t$ curves.

4. The chamber was closed and a test started. Data were recorded right after the specimen got in contact with the liquid. Measurement lasted a period of time ranging from 40 s to 120 s. This time, which depends on soil type, was determined by trial tests.

5. Step 4 was repeated for another test. If a different test liquid was used, rinsing the vessel with acetone was necessary.

6. After an experiment, all tubes were cleaned and dried. Data were obtained for analysis.

For the modified CRM, the value of κ was obtained by using a nonlinear least squares curve fit regime. MATLAB code was developed to automate the data processing and eliminate subjective factors.

Typical comparisons between measured and fitted $m-t$ curves are illustrated in Figure 5. As can be seen, the fitted results match very well with the measured data: the measured and fitted curves almost coincide. This finding in turn proves that the solution to the governing equation for the modified CRM well describes the dynamics of capillary rise. The average apparent contact angle for the soil was measured as 89.43 degrees.

Theory

The model proposed by Konrad and Morgenstern provided cold regions engineers with a good approach for frost heave predictions (22–24). The model predicts the thermally induced water flux by introducing an experimental relationship. A parameter, the segregation potential, was suggested to quantify this experimental relationship. This study presents a detailed physical explanation for the segregation potential. A new theory is proposed for the calculation of this parameter based on some fundamental soil properties. Part of the theory was briefly mentioned in a previous study by Liu et al. (41). The detailed theory is introduced in this section.

The rate of frost heave is controlled by both heat transfer and water migration in frozen soils. These two mechanisms were essentially linked by the thermodynamic equilibrium at the water–ice interface. Of special interest is the frozen fringe, for which the segregation potential is defined to represent the linear relationship between the water intake rate and the temperature gradient across the frozen

fringe. Therefore, in order to obtain a theoretical formulation for the segregation potential, it is necessary to establish a governing equation for water migration in which the accumulation of water and ice is related to temperature.

The mixed-type Richards equation is first introduced to describe the fluid movement in variably unsaturated porous media. A term related to ice formation is added to the left-hand side to extend the Richards equation to the investigation of freezing soils:

$$\underbrace{\frac{\partial \theta_w}{\partial t} + \frac{\rho_i}{\rho_w} \frac{\partial \theta_i}{\partial t}}_{\text{accumulation}} = - \underbrace{\frac{\partial}{\partial x} \left[\frac{K}{\rho_w g} \left(\frac{\partial \psi}{\partial x} - 1 \right) \right]}_{\text{flux}} \quad (25)$$

where

θ_w = volumetric water content (more specifically, unfrozen water content throughout this discussion),

ρ_w = density of water,

ρ_i = density of ice,

θ_i = volumetric ice content,

t = time,

K = hydraulic conductivity,

g = gravitational acceleration, and

ψ = soil suction.

The 1 in Equation 25 allows for the influence of gravity on water migration.

The soil suction can be related to temperature by using the Clapeyron equation. A generalized form of the Clapeyron equation is

$$\frac{d\psi}{dT} = - \frac{\rho_w L}{T} \quad (26)$$

where L is the latent heat of the phase change of water. The generalized Clapeyron equation can be integrated into the following form. Equation 27 predicts that the freezing point of water will decrease to somewhat below the freezing point of bulk water because of the presence of suction.

$$\psi = -\rho_w L \ln \frac{T}{T_0} \quad (27)$$

where T_0 is the freezing point of bulk water (in kelvins) under standard atmospheric pressure. Equation 27 was obtained on the basis of the original equation (9, 11) by assuming that the ice pressure is zero, which is more a rule than an exception when ice lenses are lacking and the osmotic effect is negligible. Another assumption is that the freezing or drying process is comparatively slow so that thermodynamic equilibrium can be ensured on the water–ice interface.

By substituting Equation 27 into Equation 25, the governing equation is reformatted as follows:

$$\underbrace{\frac{\partial \theta_w}{\partial t} + \frac{\rho_i}{\rho_w} \frac{\partial \theta_i}{\partial t}}_{\text{accumulation}} = - \underbrace{\frac{\partial}{\partial x} \left[\left(\frac{KL}{g} \frac{1}{T} \right) \frac{\partial T}{\partial x} + \frac{K}{\rho_w g} \right]}_{\text{flux}} \quad (28)$$

Therefore, the water flux caused by temperature gradients is

$$J = \left(\frac{KL}{g} \frac{1}{T} \right) \frac{\partial T}{\partial x} + \frac{K}{\rho_w g} \quad (29)$$

There are two unknowns in the Equation 29, K and T . However, K is dependent on S (42) and can be expressed as follows (43):

$$K = K_0 K_r = K_0 S^{1/2} \left[1 - (1 - S^{1/m})^m \right]^2 \quad (30)$$

where

- K_0 = hydraulic conductivity under unfrozen conditions,
- m = fitting constant, and
- S = saturation in freezing–thawing process, that is, ratio of volumetric unfrozen water content to porosity (total volume ratio of unfrozen and frozen water).

In view of the similarity between the freezing and drying processes, those equations proposed for the soil water characteristic curve can also be used for the prediction of the soil freezing characteristic curve. The equation suggested by van Genuchten (43) was adopted in this study:

$$S = \left[\frac{1}{1 + (\alpha \Psi)^n} \right]^m \quad (31)$$

where α and n are fitting constants. By combining Equations 27, 30, and 31, one obtains

$$K = K_0 K_r = K_0 \left[\frac{1}{1 + \left(-\alpha \rho_w L \ln \frac{T}{T_0} \right)^n} \right]^{\frac{m}{2}} \times \left[1 - \left(1 - \frac{1}{1 + \left(-\alpha \rho_w L \ln \frac{T}{T_0} \right)^n} \right)^m \right]^2 \quad (32)$$

As can be seen in Equation 32, K is a function of T . The physical representation of the segregation potential proposed by Konrad and Morgenstern can be obtained by integrating Equation 29 over the frozen fringe (22). If the influence of gravity is neglected, the segregation potential is

$$SP = \frac{l}{T_i - T_s} \frac{1}{l} \int_{x_s}^{x_s+l} J dx = \frac{l}{T_i - T_s} \int_{T_s}^{T_i} \left[\frac{K(T)L}{g} \frac{1}{T} \right] dT \quad (33)$$

where

- SP = segregation potential;
- T_s, T_i = temperature on top and base of frozen fringe, respectively;
- x_s = ordinate of top of frozen fringe; and
- l = length of frozen fringe.

As stated by Konrad and Morgenstern, the segregation potential is dependent on the hydraulic conductivity and the segregation-freezing temperature (22). This statement is well supported by Equation 33.

Validation of Proposed Theory

Equation 33 presents the accurate mathematical formulation for the segregation potential. The equation was simplified to verify its

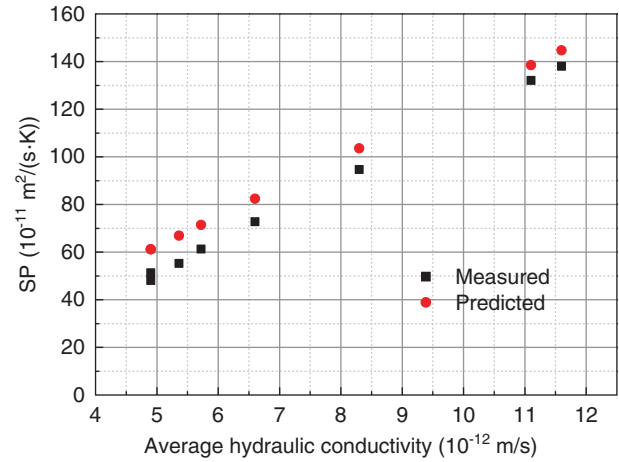


FIGURE 6 Comparison between measured and predicted SP.

validity. For the purpose, the average hydraulic conductivity of the frozen fringe, \bar{K} , was adopted; then the segregation potential can be reduced to the following form:

$$SP = \frac{\bar{K}L}{g} \frac{1}{T_s} \quad (34)$$

Equation 34 was used to predict SP with the average hydraulic conductivity obtained by Konrad and Morgenstern (23). As demonstrated in Figure 6, the predicted values are very close to the measured values. Moreover, the pattern of the variation of SP with \bar{K} predicted by Equation 34 compares very well with experimental results (23). The good comparison can hardly be a coincidence considering the small order of SP [10^{-11} m²/(s·K)] and the similar patterns between measured and predicted results. The difference between measured and predicted results is estimated to be caused by two factors: (a) the replacement of hydraulic conductivity at the top of the specimen sample with the average value of the frozen fringe and (b) the assumption that the temperature distribution over the frozen fringe is linear.

Auxiliary Relationships for SP Prediction

Additional information is required for applying Equation 33 for accurate SP prediction. This information includes the mathematical expression of $K(T)$ and the temperature on the top and base of the frozen fringe. To be more specific, five constants need to be identified: α and m, n, T_s , and T_i . This study suggests obtaining α and m, n , and T_i by fitting the phase composition curve, and it is proposed that T_s be predicted with a poroelastic approach.

The theoretical formulation for the phase composition curve can be obtained by combining Equations 27 and 31:

$$T = T(S) = T_0 \exp \left[-\frac{1}{\alpha \rho_w L} \left(S^{-\frac{1}{m}} - 1 \right)^{\frac{1}{n}} \right] \quad (35)$$

Equation 35 predicts the relationship between temperature and saturation in frozen soils that are either saturated or unsaturated under unfrozen conditions. However, the temperature for zero saturation

usually cannot be achieved by most experiments on phase composition curves. In fact, a temperature that is several kelvins below the freezing point of bulk water is usually used as the lowest temperature. However, most experiments assumed that all of the water had turned into ice at this lowest temperature. This assumption makes the measured saturation different from the true saturation used in Equation 35. In addition, the unsaturated condition under unfrozen conditions needs to be taken into account because, in many cases, saturation is measured with reference to the water content under frozen conditions. Even if a fully saturated specimen is claimed to be used, the slight unsaturated condition will also result in a difference between the measured and the true saturation. On the basis of the foregoing concerns, the measured saturation in the phase composition curve can be related to the true saturation as

$$S_M = \frac{S - S_L}{S_H - S_L} \tag{36}$$

where S_M and S are the measured saturation and true saturation, respectively, and S_L and S_H are the lowest and highest saturation achieved by the experiment, respectively. Hence the true saturation can be expressed by the measured value as

$$S = S_M S_H - S_M S_L + S_L \tag{37}$$

Substituting Equation 37 into Equation 35 yields the prediction equation for the phase composition curve:

$$T(S) = 273.15 \exp \left\{ -\frac{1}{3.34 \times 10^8 \alpha} \left[(S_M S_H - S_M S_L + S_L)^{-\frac{1}{m}} - 1 \right]^n \right\} \tag{38}$$

where T_0 is 273.15°K, L is 3.34×10^5 J/kg, and ρ_w is density of water, 1,000 kg/m³.

A thermo-time-domain reflectometry sensor was used in a previous study by Liu et al. to measure the phase composition curve of a typical subgrade soil in the state of Ohio (41).

Shown in Figure 7 is the comparison between the measured and fitted phase composition curves. The validity of the measured phase

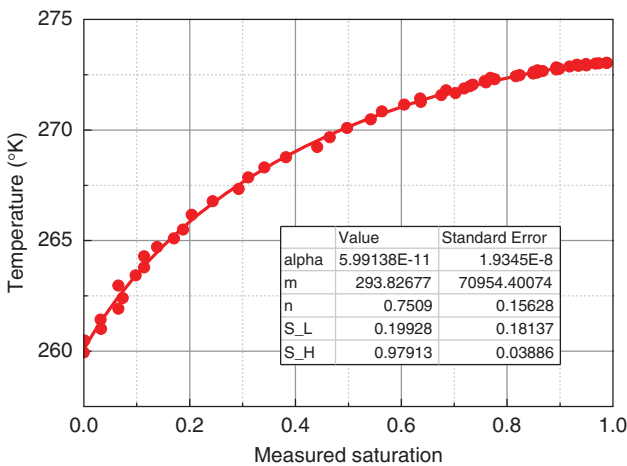


FIGURE 7 Comparison between measured and fitted phase composition curves for typical subgrade soil.

composition curve was proved by Liu et al. (41). The curve fitting was conducted with a data analysis package, Origin. As can be seen, the proposed prediction equation offered very good predictions in the whole range of measured data. The water saturation under unfrozen conditions was estimated to be 97.91%. The temperature at the base of the frozen fringe can be calculated using the following equation:

$$T_i = T_0 \exp \left[-\frac{1}{\alpha \rho_w L} (S_H^{-1/m} - 1)^n \right] \tag{39}$$

The poroelastic approach for the prediction of the segregation-freezing temperature is established on the basis of one classic constitutive relation:

$$\sigma = K_b \epsilon_v - Bp \tag{40}$$

where

- σ = isotropic pressure,
- K_b = bulk modulus,
- ϵ_v = volumetric strain,
- B = Biot–Willis coefficient, and
- p = liquid pressure.

By applying Equation 40 to saturated freezing soils and assuming that expansion in the gravitational direction is not constrained, the criterion for ice lens initiation can be obtained:

$$\sigma = BS\psi - 3K_b(0.09S) - \rho gh > 0 \text{ (tension)} \tag{41}$$

By substituting Equation 27 into the Equation 41, the segregation-freezing temperature is obtained when the skeleton pressure is zero:

$$T_s = T_0 \exp \left(\frac{-0.27K_b S - \rho gh}{\rho_w LBS} \right) \tag{42}$$

CONCLUSIONS

Thermally induced water flux is one of the most important couplings of the thermohydrromechanical processes in soils. As an essential knowledge base for studying the influence of thermal changes on engineering behaviors of soils, it has been receiving a tremendous amount of research. Among the research, the model proposed by Philip and de Vries (1) and that by Konrad and Morgenstern (22–24) have gained popularity for soils without (frozen or unfrozen) and with ice lenses, respectively. This study presents a comprehensive look at thermally induced water flux. For conditions without ice lenses, either frozen or unfrozen, the underestimation of water flux by the model of Philip and de Vries (1) is tackled with a proposed theory. Experiments with a modified CRM are suggested to help calculate the gain factor, which is used to allow for the underestimation. For thermally induced flux in freezing soils with ice lenses, the theoretical formulation for segregation potential, which is the key parameter in the model of Konrad and Morgenstern (22–24), is derived. This theoretical formulation, which is lacking in previous research, is expressed in a simple mathematical form and is proved to accurately predict the segregation potential. More auxiliary relationships are presented for calculating the segregation potential with basic soil properties and with the phase composition curve measured with a thermo–thermo-time-domain reflectometry sensor.

REFERENCES

1. Philip, J. R., and D. A. de Vries. Moisture Movement in Porous Materials under Temperature Gradients. *Transactions of the American Geophysical Union*, Vol. 38, No. 2, 1957, pp. 222–232.
2. Dirksen, C., and R. D. Miller. Closed-System Freezing of Unsaturated Soil. *Soil Science Society of America Proceedings*, Vol. 30, No. 2, 1966, pp. 168–173.
3. Nimmo, J. R., and E. E. Miller. The Temperature Dependence of Isothermal Moisture Versus Potential Characteristics of Soils. *Soil Science Society of America Journal*, Vol. 50, No. 5, 1986, pp. 1105–1113.
4. Grant, S. A., and A. Salehzadeh. Calculation of Temperature Effects on Wetting Coefficients of Porous Solids and Their Capillary Pressure Functions. *Water Resources Research*, Vol. 32, No. 2, 1996, pp. 261–270.
5. Grant, S. A., and J. Bachmann. Effect of Temperature on Capillary Pressure. *Geophysical Monograph*, Vol. 129, 2002, pp. 199–212.
6. Tuller, M., D. Or, and L. M. Dudley. Adsorption and Capillary Condensation in Porous Media: Liquid Retention and Interfacial Configurations in Angular Pores. *Water Resources Research*, Vol. 35, No. 7, 1999, pp. 1949–1964.
7. Bachmann, J., and R. R. van der Ploeg. A Review on Recent Developments in Soil Water Retention Theory: Interfacial Tension and Temperature Effects. *Journal of Plant Nutrition and Soil Science*, Vol. 165, No. 4, 2002, pp. 468–478.
8. Coussy, O. Poromechanics of Freezing Materials. *Journal of Mechanics and Physics of Solids*, Vol. 53, No. 8, 2005, pp. 1689–1718.
9. Taylor, S. A., and J. W. Cary. Linear Equations for the Simultaneous Flow of Matter and Energy in a Continuous Soil System. *Soil Science Society of America Proceedings*, Vol. 28, No. 2, 1964, pp. 167–172.
10. Cary, J. W. Water Flux in Moist Soil: Thermal Versus Suction Gradients. *Soil Science*, Vol. 100, No. 3, 1965, pp. 168–175.
11. Groenevelt, P. H., and B. D. Kay. On the Interaction of Water and Heat Transport in Frozen and Unfrozen Soils: II. The Liquid Phase. *Soil Science Society of America Proceedings*, Vol. 38, 1974, pp. 400–404.
12. Kay, B. D., and P. H. Groenevelt. On the Interaction of Water and Heat Transport in Frozen and Unfrozen soils: I. Basic Theory: The Vapor Phase. *Soil Science Society of America Proceedings*, Vol. 38, No. 3, 1974, pp. 395–400.
13. Harlan, R. L. Analysis of Coupled Heat-Fluid Transport in Partially Frozen Soil. *Water Resources Research*, Vol. 9, No. 5, 1973, pp. 1314–1323.
14. Guymon, G. L., and J. N. Luthin. A Coupled Heat and Moisture Transport Model for Arctic Soils. *Water Resources Research*, Vol. 10, No. 5, 1974, pp. 995–1001.
15. Noborio, K., K. J. McInnes, and J. L. Heilman. Two-Dimensional Model for Water, Heat and Solute Transport in Furrow-Irrigated Soil: I. Theory. *Soil Science Society of America Journal*, Vol. 60, No. 4, 1996, pp. 1001–1009.
16. Hansson, K., J. Simunek, M. Mizoguchi, L. C. Lundin, and M. T. van Genuchten. Water Flow and Heat Transport in Frozen Soil: Numerical Solution and Freeze-Thaw Applications. *Vadose Zone Journal*, Vol. 3, No. 2, 2004, pp. 693–704.
17. Thomas, H. R., P. Cleall, Y. C. Li, C. Harris, and M. Kern-Luetschg. Modelling of Cryogenic Processes in Permafrost and Seasonally Frozen Soils. *Geotechnique*, Vol. 59, No. 3, 2009, pp. 173–184.
18. Miller, R. D. Frost Heaving in Non-Colloidal Soils. In *Proc., 3rd International Conference on Permafrost*, National Research Council of Canada, Ottawa, 1978, pp. 708–713.
19. Horiguchi, K., and R. D. Miller. Experimental Studies with Frozen Soil in an “Ice Sandwich” Permeameter. *Cold Regions Science and Technology*, Vol. 3, No. 2–3, 1980, pp. 177–183.
20. Gilpin, R. R. A Model for the Prediction of Ice Lensing and Frost Heave in Soils. *Water Resources Research*, Vol. 16, No. 5, 1980, pp. 918–930.
21. Dash, J. G. Thermomolecular Pressure in Surface Melting: Motivation for Frost Heave. *Science*, Vol. 246, No. 4937, 1989, pp. 1591–1593.
22. Konrad, J. M., and N. R. Morgenstern. A Mechanistic Theory of Ice Lens Formation in Fine-Grained Soils. *Canadian Geotechnical Journal*, Vol. 17, No. 4, 1980, pp. 473–486.
23. Konrad, J. M., and N. R. Morgenstern. The Segregation Potential of a Freezing Soil. *Canadian Geotechnical Journal*, Vol. 18, No. 4, 1981, pp. 482–491.
24. Konrad, J. M., and N. R. Morgenstern. Prediction of Frost Heave in the Laboratory during Transient Freezing. *Canadian Geotechnical Journal*, Vol. 19, No. 3, 1982, pp. 250–259.
25. Constantz, J. Comparison of Isothermal and Isobaric Water Retention Paths in Nonswelling Porous Materials. *Water Resources Research*, Vol. 27, No. 12, 1991, pp. 3165–3170.
26. Noborio, K., K. J. McInnes, and J. L. Heilman. Two-Dimensional Model for Water, Heat, and Solute Transport in Furrow-Irrigated Soil: II. Field Evaluation. *Soil Science Society of America Journal*, Vol. 60, No. 4, 1996, pp. 1010–1021.
27. Cary, J. W. Soil Moisture Transport Due to Thermal Gradients: Practical Aspects. *Soil Science Society of America Proceedings*, Vol. 30, No. 4, 1966, pp. 428–433.
28. Neumann, A. W., G. Haage, and D. Renzow. The Temperature Dependence of Contact Angles of Polytetrafluoroethylene/N-alkanes. *Journal of Colloid Interface Science*, Vol. 35, No. 3, 1971, pp. 379–385.
29. Adamson, A. W. Potential Distortion Model for Contact Angle and Spreading, II: Temperature Dependent Effects. *Journal of Colloid Interface Science*, Vol. 44, No. 2, 1973, pp. 273–281.
30. Bernardin, J. D., I. Mudawar, C. B. Walsh, and E. I. Franses. Contact Angle Temperature Dependence for Water Droplets on Practical Aluminum Surfaces. *International Journal of Heat and Mass Transfer*, Vol. 40, No. 5, 1997, pp. 1017–1033.
31. Washburn, E. W. The Dynamics of Capillary Flow. *The Physical Review*, Vol. 18, No. 3, 1921, pp. 273–283.
32. Adamson, A. W. *Physical Chemistry of Surfaces*, 5th ed. John Wiley & Sons, New York, 1990.
33. Fries, N., and M. Dreyer. The Transition from Inertial to Viscous Flow in Capillary Rise. *Journal of Colloid and Interface Science*, Vol. 327, No. 1, 2008, pp. 125–128.
34. Siebold, A., A. Walliser, M. Nardin, M. Oppliger, and J. Schultz. Capillary Rise for Thermodynamic Characterization of Solid Particle Surface. *Journal of Colloid and Interface Science*, Vol. 186, No. 1, 1997, pp. 60–70.
35. Barry, D. A., J.-Y. Parlange, L. Li, H. Prommer, C. J. Cunningham, and F. Stagnitti. Analytical Approximations for Real Values of the Lambert W-function. *Mathematics and Computers in Simulation*, Vol. 53, No. 1–2, 2000, pp. 95–103.
36. Czachor, H. Modelling the Effect of Pore Structure and Wetting Angles on Capillary Rise in Soils Having Different Wettabilities. *Journal of Hydrology*, Vol. 328, No. 3–4, 2006, pp. 604–613.
37. Dullien, F. A. L., M. S. El-Sayed, and V. K. Batra. Rate of Capillary Rise in Porous Media with Nonuniform Pores. *Journal of Colloid Science*, Vol. 60, No. 3, 1977, pp. 497–506.
38. Vorvort, R. W., and S. R. Cattle. Linking Hydraulic Conductivity and Tortuosity Parameters to Pore Space Geometry and Pore-Size Distribution. *Journal of Hydrology*, Vol. 272, No. 1–4, 2003, pp. 36–49.
39. Gurau, V., and J. A. Mann. Technique for Characterization of the Wettability Properties of Gas Diffusion Media for Proton Exchange Membrane Fuel Cells. *Journal of Colloid and Interface Science*, Vol. 350, No. 2, 2010, pp. 577–580.
40. *Krüss Tensiometer 100 Instruction Manual V020715*. Krüss GmbH, Hamburg, Germany, 2001.
41. Liu, Z., X. Yu, Y. Sun, and B. Zhang. Formulation and Characterization of Freezing Saturated Soils. *Journal of Cold Regions Engineering*, Vol. 27, No. 2, 2013, pp. 94–107.
42. Fredlund, D. G., and A. Xing. Equations for the Soil-Water Characteristic Curve. *Canadian Geotechnical Journal*, Vol. 31, No. 4, 1994, pp. 521–532.
43. van Genuchten, M. T. A Close-Form Equation for Predicting the Hydraulic Conductivity of Unsaturated Soil. *Soil Science Society of America Journal*, Vol. 44, No. 5, 1980, pp. 892–898.

The Physicochemical and Biological Processes in Soils Committee peer-reviewed this paper.